Earthquakes and Structures, *Vol. 14, No. 5 (2018) 477-492*
DOI: https://doi.org/10.12989/eas.2018.14.5.477

A stochastic adaptive pushover procedure for seismic assessment of buildings

Mohammad Jafari[a] and Masoud Soltani*

Faculty of Civil and Environmental Engineering, Tarbiat Modares University, Tehran, Iran

(Received April 27, 2017, Revised March 31, 2018, Accepted April 16, 2018)

Abstract. Recently, the adaptive nonlinear static analysis method has been widely used in the field of performance based earthquake engineering. However, the proposed methods are almost deterministic and cannot directly consider the seismic record uncertainties. In the current study an innovative Stochastic Adaptive Pushover Analysis, called "SAPA", based on equivalent hysteresis system responses is developed to consider the earthquake record to record uncertainties. The methodology offers a direct stochastic analysis which estimates the seismic demands of the structure in a probabilistic manner. In this procedure by using a stochastic linearization technique in each step, the equivalent hysteresis system is analyzed and the probabilistic characteristics of the result are obtained by which the lateral force pattern is extracted and the actual structure is pushed. To compare the results, three different types of analysis have been considered; conventional pushover methods, incremental dynamic analysis, IDA, and the SAPA method. The result shows an admirable accuracy in predicting the structure responses.

Keywords: Bouc-Wen model; stochastic adaptive pushover; stochastic linearization; extreme value

1. Introduction

With the increase in the use of the static pushover methods for seismic assessment and design of the structures, the investigation of the method and probing their inherent limitations and approximations became more necessary. Therefore, significant attempts at improving the procedure have been made and many researchers have contributed developments to enhance the performance of the pushover techniques. In the early proposed conventional static pushover procedures (ATC-40 1996, FEMA-356 2000, Pour *et al*. 2014), the applied lateral load profile was invariant. To overcome the certain limitations of classic method with constant load profile as it schematically shown in Fig. 1(c) (Pour *et al*. 2014), several improved pushover procedures have been proposed. However, to account for the higher modes effect some advanced multi-run modal pushover procedures based on the elastic modal decomposition ideas have been developed which first was proposed by Chopra and Goel (2002) and then used for seismic analysis of different types of structures (Poursha *et al*. 2009, Shayanfar *et al*. 2013, Tataie *et al*. 2012, Sarkar *et al*. 2013). In order to consider the effect of progressive structural stiffness degradation, the Adaptive Pushover methods were proposed (Fig. 1(a)). It is necessary to mention that these adaptive methods, mostly lead to the increase in complexity of the analyses which sometimes make them inappropriate for first stage design or rehabilitation. In the other words, increasing the complexity of the Push-Over method, deprives it from its main advantage i.e., its simplicity (Baros and Anagnostopoulos 2017, Baros and Dritsos 2008, Anagnostopoulos *et al*. 2015), which makes it more appropriate for research tools rather than a simple design tool.

Bracci *et al*. (1997), Reinhorn and Calvi (1997) proposed to update the force distribution as a function of base and floor shears at the previous load step. A different adaptive procedure was proposed by Gupta and Kunnath (2000) involving, separate pushover analysis for each mode where the results for different modes were combined by certain combination rule. Furthermore, Kalkan and Kunnath (2006) proposed an enhanced procedure, called Adaptive Modal Combination, which combines the adaptive pushover analysis suggested by Gupta and Kunnath (2000) and the MPA suggested by Chopra and Goel (2002). However, the method is based on the assumption that the effects of various modes in the nonlinear range are uncoupled, just as in elastic modal analysis. The adaptive pushover method proposed by Elnashai (2001) is theoretically similar to the suggestions of Reinhorn (1997), with the main difference that the adaptive algorithm was implemented in a distributed inelasticity fiber finite element code. Moreover, Antoniou and Pinho (2004) proposed an adaptive procedure where the loading pattern is based on displacements of the stories. In order to increase the efficiency of the aforementioned advanced push over method, recently some alterations were made (Landi *et al*. 2014, Araújo *et al*. 2014, Tarbali and Shakeri 2014, Beheshti-Aval and Jahanfekr 2015). However, despite such an apparent improvement, all of the aforementioned methods are deterministic and none of them are capable of directly addressing the records uncertainty in the analysis process.

Unfortunately, the subject of seismic demand uncertainty is not comprehensively discussed in the

*Corresponding author, Associate Professor
E-mail: msoltani@modares.ac.ir
[a]Ph.D. Student
E-mail: mohammad.jafari@modares.ac.ir

http://www.techno-press.com/journals/eas&subpage=7 ISSN: 2092-7614 (Print), 2092-7622 (Online)

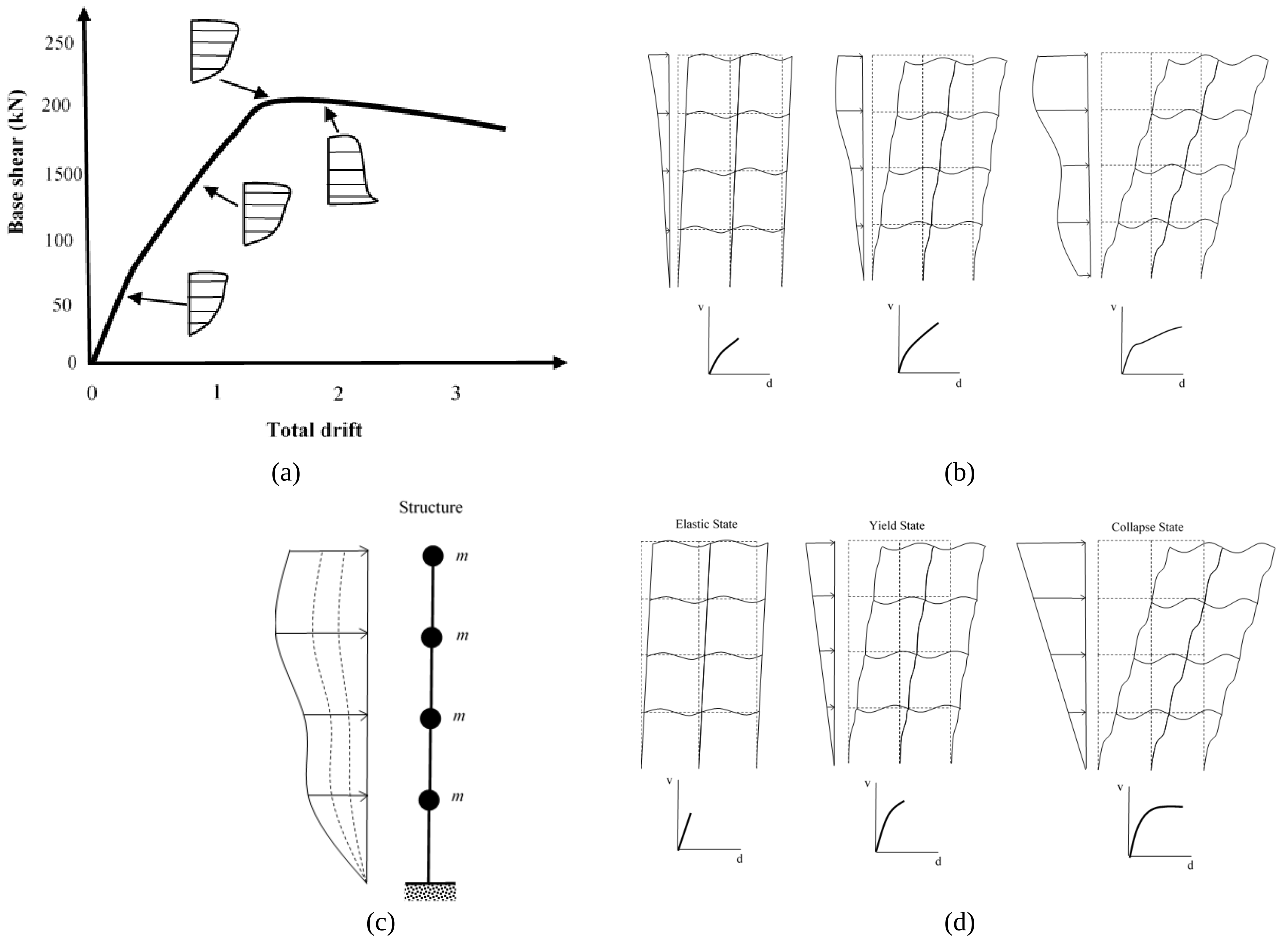

Fig. 1 Lateral load profile. (a) Schematic deformation of the lateral force profile in each step. (b) Structural deformation and its capacity curve in adaptive push over analysis. (c) Applying constant lateral force profile. (d) Structural deformation and its capacity curve under constant load profile

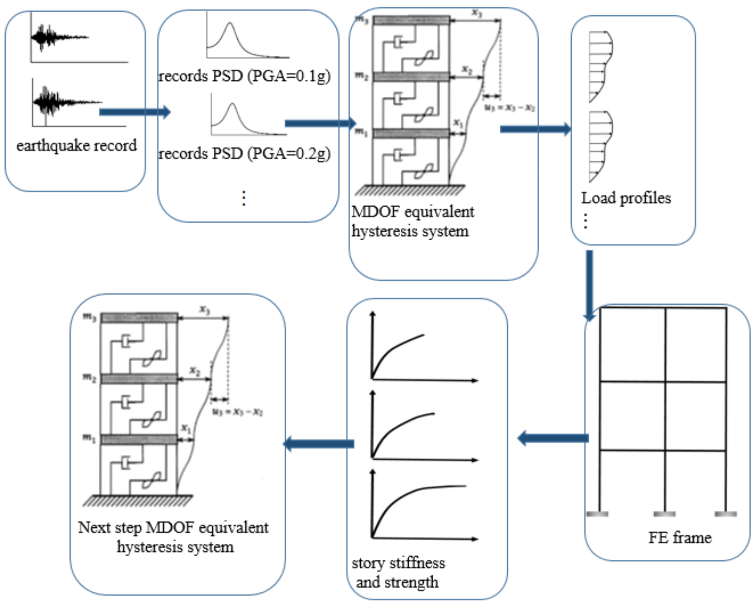

Fig. 2 The general steps of the SAPA method

literature. Monte-Carlo simulation methods are powerful tools that can deal with almost any problem and handle the uncertainties involved, but this always comes at the cost of a great number of intensive nonlinear dynamic analysis computational efforts. For earthquake engineering problems, one of the most comprehensive methods to deal with the uncertainties in seismic records is the Incremental Dynamic Analysis, IDA, proposed by Vamvatsikos and Cornell (2002), which requires multiple nonlinear dynamic analyses.

The development of the proposed SAPA procedure is motivated by the need of eliminating the drawbacks of the deterministic methods. In fact, to overcome the computational obstacle and reserve the conceptual superiority of nonlinear dynamic method which can deal with earthquake record uncertainties and without necessarily omitting any useful feature of the nonlinear static analysis method, using an equivalent hysteresis system and linearization technique, a new stochastic analysis procedure is developed, by which the structural seismic demands are estimated (Fig. 2). It is necessary to mention that the proposed method is somehow complicated which is in contrast with the philosophy of the pushover method as a simple process. Thus, it should not be considered as an alternative method for the current codes of practice, but if the proposed algorithm is implemented in a computer program, there seems to be no difference for users who use them.

2. Stochastic adaptive pushover analysis based on equivalent hysteresis system responses

To evaluate the seismic demands of structures using the SAPA method, a step-by-step procedure is presented in this section. This procedure is basically related to the linearization of the equivalent hysteresis system with respect to progressive increment of the applied base excitation. The proposed procedure consists of the following steps (Fig. 3):

(i). Evaluating the power spectral density (PSD) of the records and scaling the base excitation: In this study, the analyses are conducted in the frequency domain. Hence, in the incremental stochastic nonlinear analysis, the PSD of the records are incrementally scaled and applied simultaneously to the hysteresis structure as a base excitation.

Since earthquakes are best simulated by nonstationary filtered white noise where the power Associated with frequencies and randomness can be incorporated, the synthetic records used in this analysis were generated using PSD function. In order to validate the result in frequency domain, the Monte Carlo analysis in time domain is used for each step, in which an ensemble of artificial earthquake records produced from the corresponding PSD intensity are chosen as a base excitation. The ground acceleration ($\ddot{u}_g$), is expressed in the following form

$$\ddot{u}_g = PGA*e(t)*X(t) \tag{1}$$

where PGA, $e(t)$, and $X(t)$ are peak ground acceleration, normalized nonstationary envelope function, and stationary filtered white noise, respectively. The ensemble $X(t)$ is represented as

$$X(t) = \sum \sqrt{2S_g(\omega_n)\Delta\omega}.\cos(\omega_n t + \theta_n) \qquad n = 1, 2, ..., m \tag{2}$$

where ω_n is frequency of n-th generated sample ($\omega_n = n\Delta\omega$), θ_n is a random phase angle of the n-th generated sample between 0 and 2π, and $S_g(\omega_n)$ is earthquake power spectral density which is expressed by Kanai (1957) and Tajimi (1967) filter as

$$S(\omega)=S_0\frac{1+\left[2\xi_g\left(\frac{\omega}{\omega_g}\right)\right]^2}{\left[1-\left(\frac{\omega}{\omega_g}\right)^2\right]^2+\left[2\xi_g\left(\frac{\omega}{\omega_g}\right)\right]^2} \tag{3}$$

where ω_g and ξ_g are dominant earthquake frequency and damping ratio of the site. The normalized nonstationary envelope (Lutes and Sarkani 2004) is considered as

$$f(t)=\frac{[e^{-at}-e^{-bt}]}{c_f} \qquad (t \succ 0) \tag{4}$$

in which a and b are constants and c_f is

$$c_f=\left[\left(\frac{a}{b}\right)^{a/(b-a)}-\left(\frac{a}{b}\right)^{b/(b-a)}\right] \tag{5}$$

The main reason that artificial earthquake records have been used in this article is that the selection of earthquake records compatible with site specific characteristic is not always possible. In addition, selecting a suite of available real records may introduce some errors in the structural demand estimation process of a newly proposed method which can be difficult to interpret. However, the method is not restricted to synthetic excitations and it can be applied for any ensemble of site specific records by using the PSD of the real earthquake records.

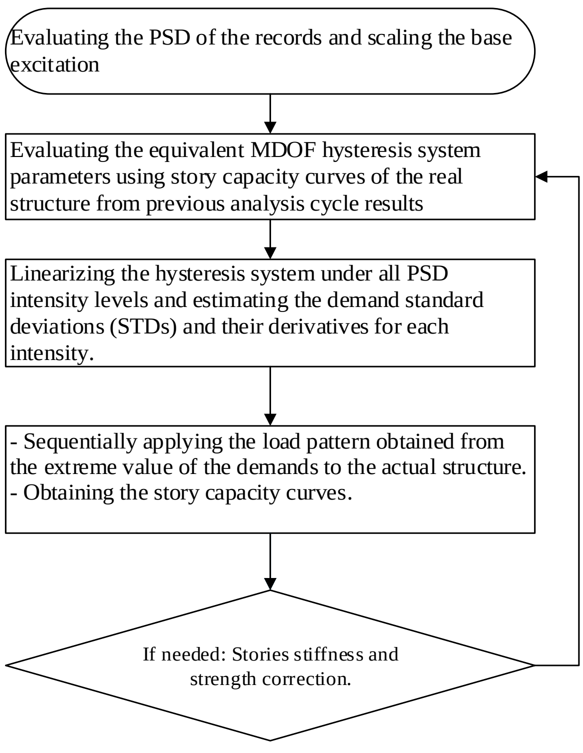

Fig. 3 Flow chart of the SAPA method.

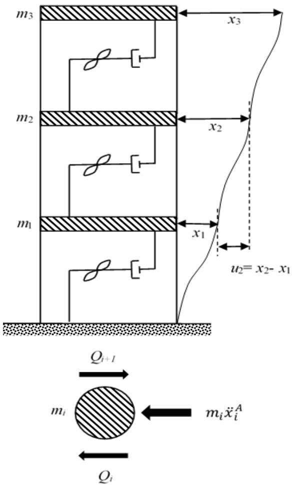

Fig. 4 The MDOF shear frame and story forces (Foliente 1993)

(ii). Evaluating the equivalent MDOF hysteresis system parameters using story capacity curves of the real structure from previous analysis cycle results:

The hysteretic restoring force model is selected as Bouc–Wen hysteresis model (Bouc 1967, Wen 1967). The model is given by the following system of equations

$$m\ddot{u}(t)+c\dot{u}(t)+R[u(t),z(t)]=F(t) \tag{6}$$

$$R[u(t),z(t)]=k_i a u(t)+(1-a)k_i z(t) \tag{7}$$

$$\dot{z}=Au-b|\dot{u}||z|^{n-1}z-g\dot{u}|z|^{n} \tag{8}$$

where $u(t)$ is system displacement, $z(t)$ is the hysteretic restoring force, m, c and k_i are mass, damping coefficient and elastic stiffness parameters, respectively; α is a ratio of post-yield to pre-yield stiffness; A, β, g, and n are parameters which regulate the shape of the hysteresis loop.

In the present study, the shear building model for MDOF system as shown in Fig. 4 is considered as the equivalent hysteresis system. The building is subjected to horizontal ground acceleration a_g. For the case of MDOF system, the story forces for i-th story are represented as

$$q_i=\alpha_i k_i u_i(t)+(1-\alpha_i)k_i z_i(t) \tag{9}$$

where the auxiliary variable z_i assigned to the i-th story is

$$\dot{z}_i=A_i u_i-\beta_i|u_i||z_i|^{n_i-1}z_i-\gamma_i\dot{u}_i|z_i|^{n_i} \tag{10}$$

and u_i is the i-th story drift as

$$u_i=d_i-d_{i-1} \tag{11}$$

with d_i representing the displacement of the i-th mass relative to the ground. Therefore, the equation of motion for the i-th mass can be written as

$$\begin{aligned} & m_i\left(\sum_{j=1}^{i}\ddot{u}_j+a_g\right)+c_i\dot{u}_i- \\ & c_{i+1}\dot{u}_{i+1}+q_i-q_{i+1}=0 \end{aligned} \tag{12}$$

where i=1,…,ND and ND is total number of discretized mass. Eq. (12) can be written in matrix form as follow

$$\begin{aligned} & [M]\{\ddot{U}\}+[C]\{\dot{U}\}+[K]\{U\} \\ & +[G]\{Z\}=-[M_0]\{I\}a_g \end{aligned} \tag{13}$$

where $\{\tilde{I}\}$ is the influence vector, and

$$\{\tilde{I}\}=\begin{Bmatrix}1\\1\\\vdots\\1\end{Bmatrix} \tag{14}$$

$$M=\begin{bmatrix} m_1 & & & 0 \\ m_2 & m_2 & & \\ \vdots & & \ddots & \\ m_{ND} & m_{ND} & \cdots & m_{ND} \end{bmatrix} \tag{15}$$

$$M_0=\begin{bmatrix} m_1 & & & 0 \\ & m_2 & & \\ & & \ddots & \\ 0 & & & m_{ND} \end{bmatrix} \tag{16}$$

$$K=\begin{bmatrix} \alpha_1k_1 & -\alpha_2k_2 & & & 0 \\ & \alpha_2k_2 & -\alpha_3k_3 & & \\ & & \ddots & & \\ & & & \alpha_{ND-1}k_{ND-1} & -\alpha_{ND}k_{ND} \\ 0 & & & & \alpha_{ND}k_{ND} \end{bmatrix} \tag{17}$$

$$G=\begin{bmatrix} (1-\alpha_1)k_1 & -(1-\alpha_2)k_2 & & & 0 \\ & (1-\alpha_2)k_2 & -(1-\alpha_3)k_3 & & \\ & & \ddots & & \\ & & & (1-\alpha_{ND-1})k_{ND-1} & -(1-\alpha_{ND})k_{ND} \\ 0 & & & & (1-\alpha_{ND})k_{ND} \end{bmatrix} \tag{18}$$

$$\{U\}=\begin{Bmatrix}u_1\\u_2\\\vdots\\u_{ND}\end{Bmatrix},\ \{Z\}=\begin{Bmatrix}z_1\\z_2\\\vdots\\z_{ND}\end{Bmatrix} \tag{19}$$

$$[C]=\alpha_c[M]+\beta_c[K_0] \tag{20}$$

According to Eq. (7) and Fig. 5, in order to proceed with the proposed pushover method at each step, the strength (F_h or F_y) equivalent n-th story Bouc-Wen model is estimated as

$$\begin{aligned} & F_h=F_y=(1-\alpha)\frac{F_y}{u_y}z(t)=(1-\alpha)\frac{F_y}{u_y}\left(\frac{A}{\gamma+\beta}\right)^{1/n} \\ & \Rightarrow\gamma+\beta=A\left(\frac{(1-\alpha)}{u_y}\right)^{n} \end{aligned} \tag{21}$$

where A=1, n=2 and α=0.03. According to Wen (1967) for reinforced concrete frame, the parameter may be considered as

$$b\succ 0;\quad b=-2g \tag{22}$$

So, having the strength and the initial stiffness of the story, the parameter of the equivalent Bouc-Wen model of

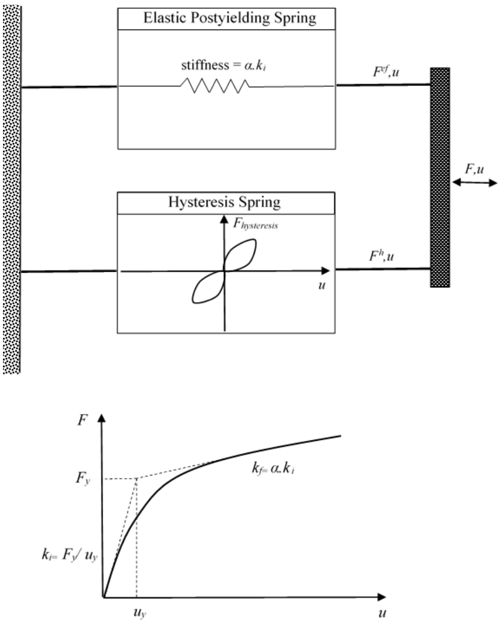

Fig. 5 Schematic representation of Bouc-Wen parameters (Charalampakis 2008)

the story can be evaluated.

(iii). Linearizing the hysteresis system under all PSD intensity levels and estimating the demand standard deviations (STDs) and their derivatives for each intensity.

Statistical linearization is used to estimate the first and the second moment of the responses of the nonlinear systems (Roberts and Spanos 2003). By minimizing the mean square error between a nonlinear system and an equivalent linear one, the linearized Bouc-wen parameters for a MDOF system are obtained as (Foliente 1993, Hurtado and Barbat 2000)

$$\{\dot{Z}\}=[C_e]\{\dot{U}\}+[K_e]\{Z\} \tag{23}$$

in which

$$\{Z\}=\begin{Bmatrix} z_1 \\ : \\ z_{ND} \end{Bmatrix}, \quad \{\dot{U}\}=\begin{Bmatrix} \dot{u}_1 \\ : \\ \dot{u}_{ND} \end{Bmatrix} \tag{24}$$

$$[C_e]=\begin{bmatrix} c_{e1} & & 0 \\ & . & \\ 0 & & c_{eND} \end{bmatrix}, [K_e]=\begin{bmatrix} k_{e1} & & 0 \\ & . & \\ 0 & & k_{eND} \end{bmatrix} \tag{25}$$

In Eq. (25) the linearization coefficients are

$$C_{ei}=A_i-\beta_i F_{1i}-\gamma_i F_{2i} \tag{26}$$

$$K_{ei}=-\beta_i F_{3i}-\gamma_i F_{4i} \tag{27}$$

where functions F_i (i=1, 2, 3, 4) are given by

$$F_1=\frac{\sigma_z^n}{\pi}\Gamma\left(\frac{n+2}{2}\right)2^{n/2} I_s \tag{28}$$

$$F_2=\frac{\sigma_z^n}{\sqrt{\pi}}\Gamma\left(\frac{n+1}{2}\right)2^{n/2} \tag{29}$$

$$F_3=\frac{n\sigma_{\dot{u}}\sigma_z^{n-1}}{\pi}\Gamma\left(\frac{n+2}{2}\right)2^{n/2}\times \left\{\frac{2(1-\rho_{\dot{u}z}^2)^{(n+1)/2}}{n}+\rho_{\dot{u}z}I_s\right\} \tag{30}$$

$$F_4=\frac{n}{\sqrt{\pi}}\rho_{\dot{u}z}\sigma_{\dot{u}}\sigma_z^{n-1}\Gamma\left(\frac{n+1}{2}\right)2^{n/2} \tag{31}$$

with

$$I_s = 2\int_l^{\pi/2}\sin^n\theta\, d\theta, \qquad l=\tan^{-1}\left(\frac{\sqrt{1-\rho_{\dot{u}z}^2}}{\rho_{\dot{u}z}^2}\right) \tag{32}$$

$$\sigma_z=\sqrt{E[z^2]},\ \sigma_{\dot{u}}=\sqrt{E[\dot{u}^2]}, \qquad \rho_{\dot{u}z}=\frac{E[\dot{u}z]}{\sqrt{E[\dot{u}^2]\,E[z^2]}} \tag{33}$$

Introducing a vector y as follow

$$y=\begin{Bmatrix} \{u\} \\ \{\dot{u}\} \\ \{z\} \end{Bmatrix}, \dot{y}=\begin{Bmatrix} \{\dot{u}\} \\ \{\ddot{u}\} \\ \{\dot{z}\} \end{Bmatrix} \tag{34}$$

$$m_i\left(\sum_{j=1}^{i}\ddot{u}_j+\ddot{x}_g\right)+c_i\dot{u}_i-c_{i+1}\dot{u}_{i+1}+ \alpha_i k_i u_i+(1-\alpha_i)k_i z_i-\alpha_{i+1}k_{i+1}u_{i+1} -(1-\alpha_{i+1})k_{i+1}z_{i+1}=0 \tag{35}$$

$$\dot{z}_i-ce_i\,\dot{u}_i-ke_i\,z_i=0 \tag{36}$$

When Eq. (37) is multiplied by y^T, the expectation operator is applied and the resulting equation is added into its transpose, the covariance equation is obtained as

$$\dot{y}+Gy=f(t) \tag{37}$$

$$\dot{y}y^T+Gyy^T=f(t)y^T \tag{38}$$

$$E[\dot{y}y^T]+E[Gyy^T]=E[f(t)y^T] \tag{39}$$

$$\dot{S}+GS+SG^T=B \tag{40}$$

$$S=E[yy^T] \tag{41}$$

$$\dot{S}=E[\dot{y}y^T] \tag{42}$$

$$B=E[yf^T]+E[fy^T] \tag{43}$$

For stationary solution Eq. (40) is solved with $\dot{S}=0$ where S is

$$S=E[y\bar{y}]=E\left\{\begin{Bmatrix} \{u\} \\ \{\dot{u}\} \\ \{z\} \end{Bmatrix}\{\{u\}\ \ \{\dot{u}\}\ \ \{z\}\}\right\} \tag{44}$$

The rearranged form of Kanai-Tajimi filter is as follow

$$\ddot{x}_f + 2\xi_g \omega_g \dot{x}_f + \omega_g^2 x_f = n(t) \tag{45}$$

$$\ddot{x}_g = -(2\xi_g \omega_g \dot{x}_f + \omega_g^2 x_f) \tag{46}$$

In which $n(t)$ is white noise. The governing equation can be reordered as

$$\begin{aligned} & m_i\left(\sum_{j=1}^{i} \ddot{u}_j\right) + c_i \dot{u}_i - c_{i+1}\dot{u}_{i+1} + \\ & \alpha_i k_i u_i + (1-\alpha_i)k_i z_i - \alpha_{i+1}k_{i+1}u_{i+1} - \\ & (1-\alpha_{i+1})k_{i+1}z_{i+1} = -(2\xi_g \omega_g \dot{x}_f + \omega_g^2 x_f) \end{aligned} \tag{47}$$

By rearranging the above equation for each story (each degree of freedom) and applying the Kanai-Tajimi filter, the Eqs. (44) and (40) parameters for MDOF system become as follow

$$\begin{aligned} & y = \begin{Bmatrix} \{u\}_{ND,1} \\ \{\dot{u}\}_{ND,1} \\ \{z\}_{ND,1} \\ x_f \\ \dot{x}_f \end{Bmatrix}, \dot{y} = \begin{Bmatrix} \{\dot{u}\}_{ND,1} \\ \{\ddot{u}\}_{ND,1} \\ \{\dot{z}\}_{ND,1} \\ \dot{x}_f \\ \ddot{x}_f \end{Bmatrix}, f(t) = \begin{Bmatrix} \{0\}_{ND,1} \\ \{0\}_{ND,1} \\ \{0\}_{ND,1} \\ 0 \\ n(t) \end{Bmatrix}, \\ & B = \begin{bmatrix} 0 & \cdots & 0 \\ \vdots & \ddots & \vdots \\ 0 & \cdots & 2\pi s_0 \end{bmatrix}_{(3ND+2)(3ND+2)} \end{aligned} \tag{48}$$

To solve Eq. (40), an iterative procedure is needed because G depends on structural system properties and linearization coefficients while these coefficients depend on the covariance S which again depends on G.

(iv). Deriving the extreme value of the demands for the considered probability by which the load profile is evaluated.

Beside the statistical characteristic of the responses, there is a need for evaluating extreme values of the seismic demands. As it is demonstrated later it is required to evaluate two sets of demands; displacement demands like maximum story drifts and roof displacements and force demands such as maximum story shear and maximum base shear. In this study, in order to evaluate the maximum demands, two types of extreme value estimation formulation have been used; the Davenport method for the displacement demands and the cross analysis method, which render a better result for force demands. The closed-form formula introduced by Davenport (1964) is widely used for estimating the mean ($\bar{U}_{st}$) and standard deviation ($\sigma\bar{U}_{st}$) of an extreme value of the structural responses.

$$\bar{U}_{st} = \left(\left[2\ln(\sqrt{1-\varepsilon^2}\,\nu T)\right]^{0.5} + \frac{\gamma}{\left[2\ln(\sqrt{1-\varepsilon^2}\,\nu T)\right]^{0.5}}\right)\sigma_u \tag{49}$$

$$\varepsilon = \sqrt{1-m_2^2/(m_0 m_4)} \ ; \quad m_i = \int_0^{\infty} (2\pi f)^i S_x(f)\,df \tag{50}$$

$$\nu = \frac{\sigma_{\dot{u}}}{2\pi\sigma_u} \tag{51}$$

where $\nu = \sigma_{\dot{u}}/2\pi\sigma_u$ is the upcrossing rate across zero mean level, m_i is the i-th spectral moment, T is the time of the records, σ_u and $\sigma_{\dot{u}}$ are the standard deviations (STDs) of the drift and drift rate for each degree of freedom, respectively which are obtained directly from linearization process, and $\gamma = 0.5727$ is the Euler's constant. In the cross analysis formulation (Lutes and Sarkani 2004) for any given probability the extreme value can be calculated according to following equation

$$\begin{aligned} & \begin{Bmatrix} P_a = 1 - e^{-\nu_a^+ T} \\ \nu_a^+ = \dfrac{1}{2\pi}\dfrac{\sigma_{\dot{y}}}{\sigma_y} e^{-a^2 / 2\sigma_y^2} \end{Bmatrix} \Rightarrow \\ & a = \left(\sqrt{-2\ln\left[\frac{-2\pi\sigma_y}{T\sigma_{\dot{y}}}\ln(1-P_a)\right]}\right)\sigma_y \end{aligned} \tag{52}$$

where a is the extreme value and P_a is the desired probability of the extreme value.

Real earthquake records are nonstationary. So, using the linearization results obtained under stationary excitations, and introducing the nonsationary envelope according to Eq. (4) the nonstationary results are obtained as follow

$$\begin{aligned} & S_{nst}(t) = \int_{-\infty}^{+\infty} H(\omega) S_F(\omega,t) H^*(\omega)\, d\omega = \\ & \eta^2(t) \int_{-\infty}^{+\infty} H(\omega) S_g(\omega) H^*(\omega)\, d\omega = \eta^2(t) S_{st} \end{aligned} \tag{53}$$

In which $H(\omega)$ is the system frequency response function. The aforementioned methods for extreme value evaluation are applicable just for the stationary demands (the STD of the quantity and its first derivative are constant and do not change by time). Therefore, the record time (T) of the nonstationary excitations and STDs of the responses are approximated by an equivalent stationary time (T_{eq}) and STDs (σ_{eq}) (Michaelov *et al.* 2001).

$$\begin{aligned} & \sigma_{eq}^2(n) = \frac{I(n+1)}{I(n)} \ ; \quad T_{eq}(n) = \frac{I(n)}{\sigma_{eq}^{2n}(n)}; \\ & I(n) = \int_0^T \sigma_{nst}^{2n}(t)\, dt = \sigma_{st}^{2n} \int_0^T \eta^{2n}(t)\, dt \end{aligned} \tag{54}$$

The approximation method is based on the approximation of the cumulative distribution function (CDF) of the extreme value of a nonstationary process by the CDF of a corresponding equivalent stationary process. To determine the value of n, one can at first compute the first approximation for σ_{eq} and a using Eqs. (52) and (54) for some arbitrary n, then choose a corrected value of n as

$$n(T,P) = \frac{a^2(T,P)}{2\sigma_{eq}^2} \tag{55}$$

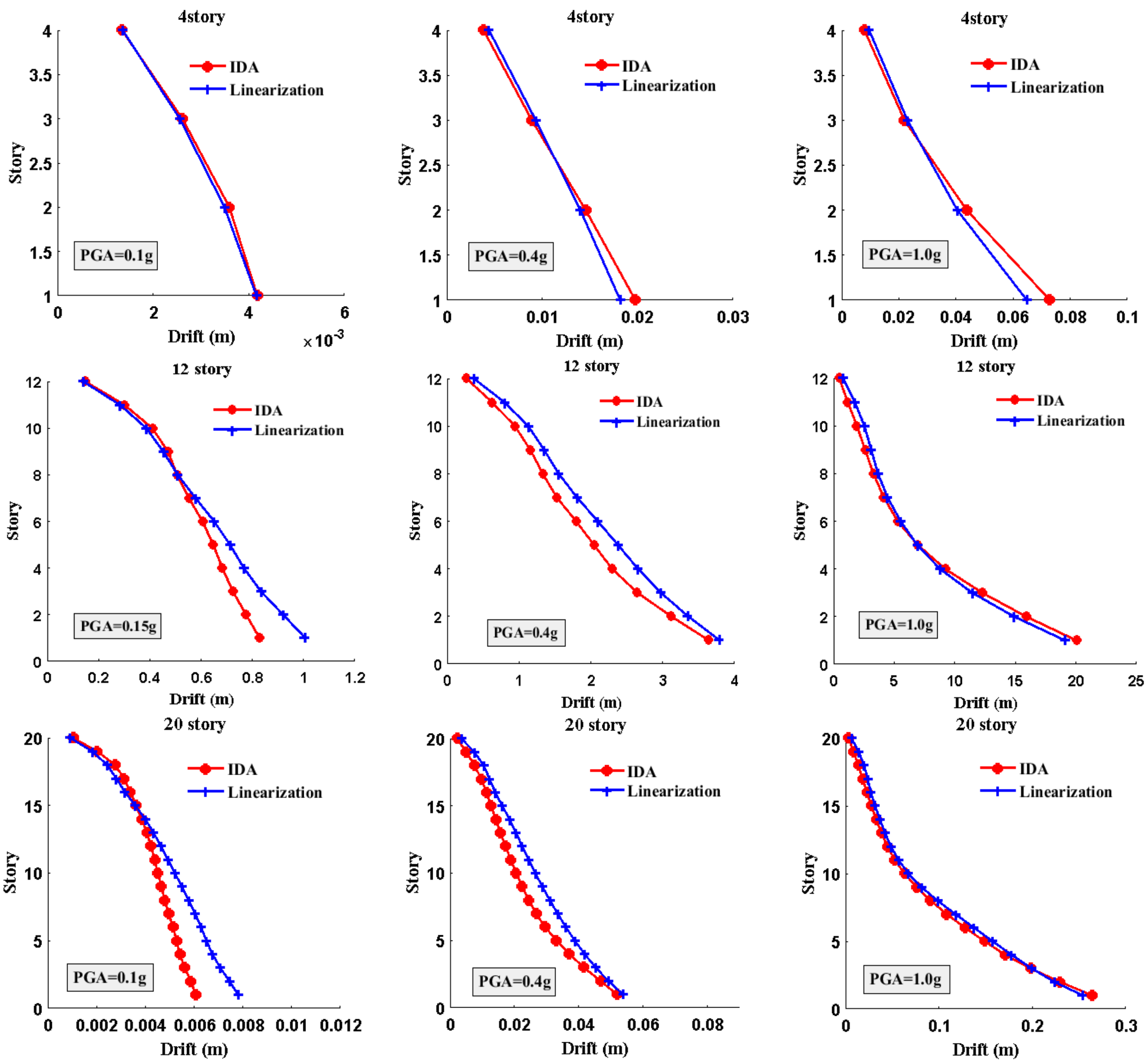

Fig. 6 Peak story drift profile resulting from IDA and linearization

Having the new n, the equivalent stationary record time and responses STDs are obtained as follow

$$\sigma_{eq}^2(n) = \frac{I(n+1)}{I(n)}\ ; \qquad T_{eq}(n) = e^n \int_0^T e^{\left(\frac{-n.\sigma_{eq}^2(n)}{\sigma_x^2(t)}\right)} dt \tag{56}$$

It is necessary to mention that this iterative process is usually converged after two or three iterations depending on the first guess of n value.

(v). sequentially applying the load pattern obtained from the extreme value of the demands to the actual structure and obtaining the story capacity curves by which an updated equivalent hysteresis system is evaluated. The lateral force profile is chosen in a way that it can produce the same maximum story drifts as obtained from step (iv).

(vi). repeating step (i) to (v) using the updated equivalent hysteresis system obtained at the end of the cycle.

The stochastic linearization procedure of the hysteresis system is verified for three levels of the typical small, medium and high-rise buildings denoted as four, twelve and twenty story two dimensional building frames (the characteristics of the frames are presented in Appendix). The proposed algorithm of the incremental stochastic analysis of the hysteresis system is written as a MATLAB computer code. The responses estimated from the proposed method are compared to those resulted from the nonlinear dynamic analysis. 100 artificial earthquake records and their PSDs are considered in this study for each step (for each intensity).

As it was noted earlier the ground motion model in frequency domain is selected as the Kanai-Tajimi PSD. According to Elgademsi (Elghadamsi *et al.* 1988) the deep

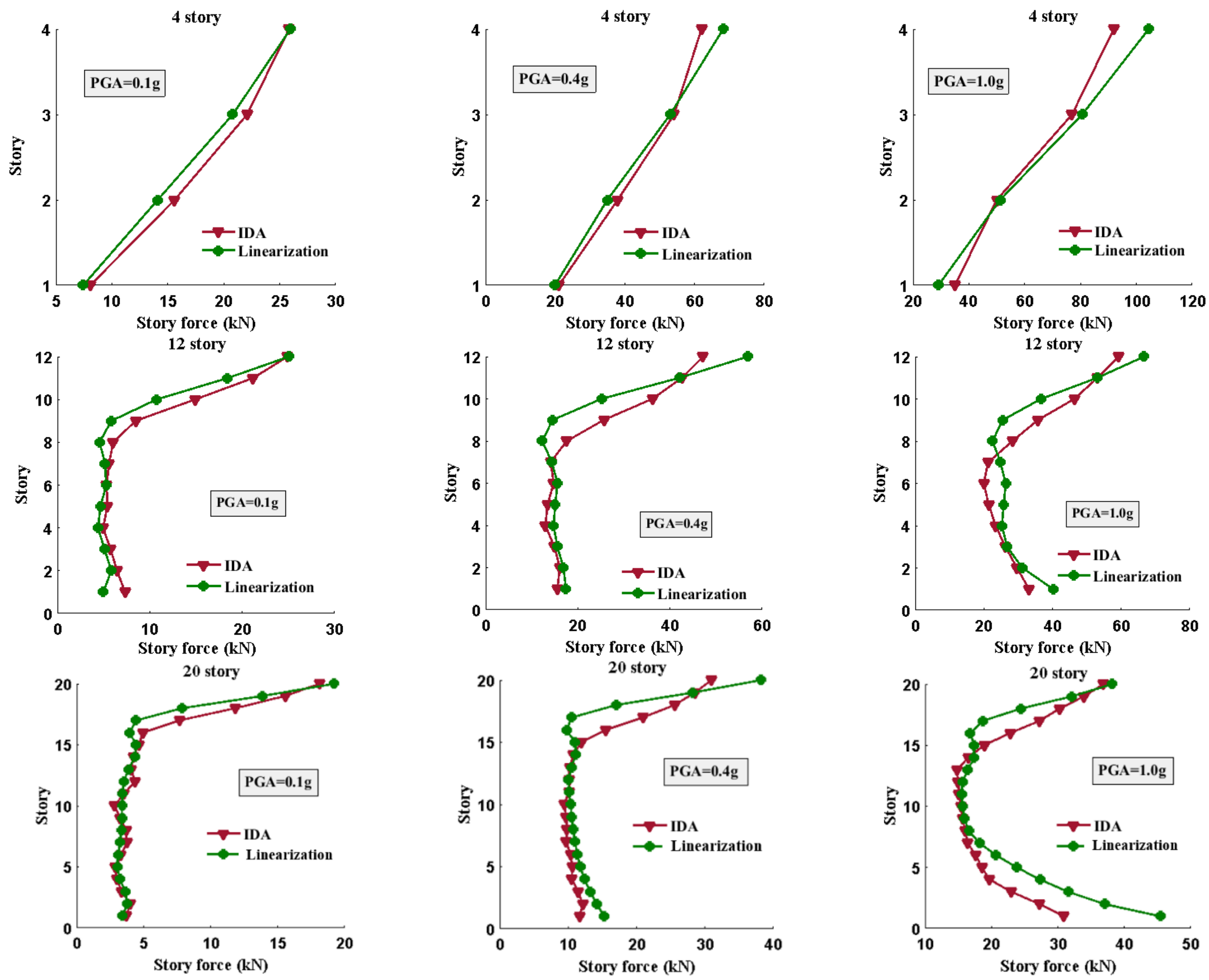

Fig. 7 Story load profiles resulting from IDA and linearization

cohesionless site conditionparameters are considered as: ω_g=18.34 (rad/sec), ξ_g=0.34, and S_0=94.76 (cm^2/sec^3).

In Figs. 6 and 7 the story drifts and force profiles resulting from IDA are compared to responses of the stochastic analyses. In all cases, at low intensity records, higher modes effect result in larger demands at the upper story level and as the intensity of the records are increased, the increase in the story drifts start to shift to lower story levels, as it is for records with 1.0 g PGA, the dynamic response of the building shows significant demand at the first story level. As for the global level results, same observation and trends apply to story levels where the comparison of story drifts and force profiles shows that although linearization method underestimates the demand for some stories and overestimate the demand for others, the variations are not significant and the general trends are almost identical.

In the linearization method, the standard deviations of the story drifts are estimated by the covariance matrix in Eq. (44) and using the extreme value formulas (Eqs. (49) and (52)) the extreme value of the drift for the preferred percentile is extracted and compared to those achieved from IDA. To make the comparison more tractable, using the story B-W models the stories shear forces were calculated from the drifts and the story forces were evaluated. In Fig. 8 the capacity curves of the structures obtained from linearization method are compared to results of dynamic analysis. It is necessary to mention that the lateral forces are obtained from the average of the maximum dynamic responses, so they resemble the average of the seismic demand. To achieve lateral forces with different probabilities, the corresponding probability of the dynamic responses should be used. Accordingly, using lateral forces obtained from dynamic response percentiles, in Fig. 9 the capacity curves of the 12 story frame are presented for different percentiles of base shear and roof displacement (denoted as V and D) and compared to capacity curves obtained from IDA. As it is shown in the Fig. 9, three types of probabilistic capacity curves are presented; (a) both base shear and roof displacement for different percentiles, (b) base shear for 50th percentile and roof displacement for different percentiles, and (c) roof displacement for 50th percentile and base shear for different percentiles. In the first type of the capacity curve, the same percentile level is applied for both of the base shear and roof displacement and as can be seen, the changes in performance levels is like changing the corresponding target displacements. On the other hand, the other capacity curves have the advantages to

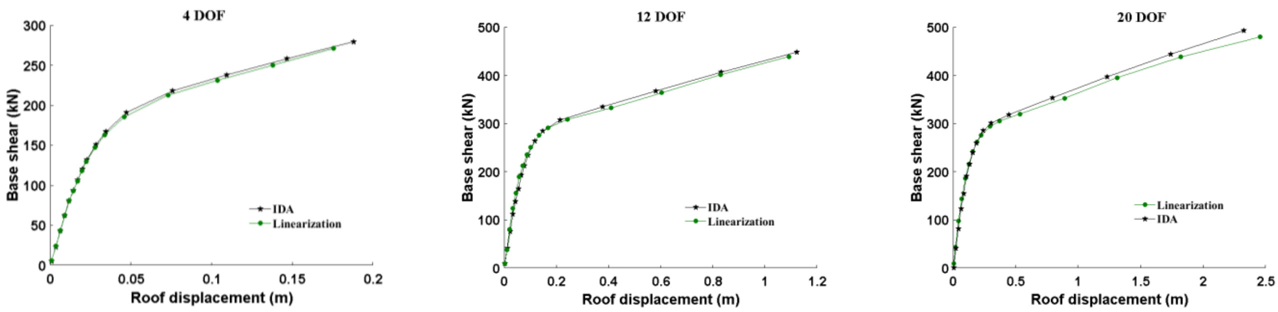

Fig. 8 Capacity curves under different excitations

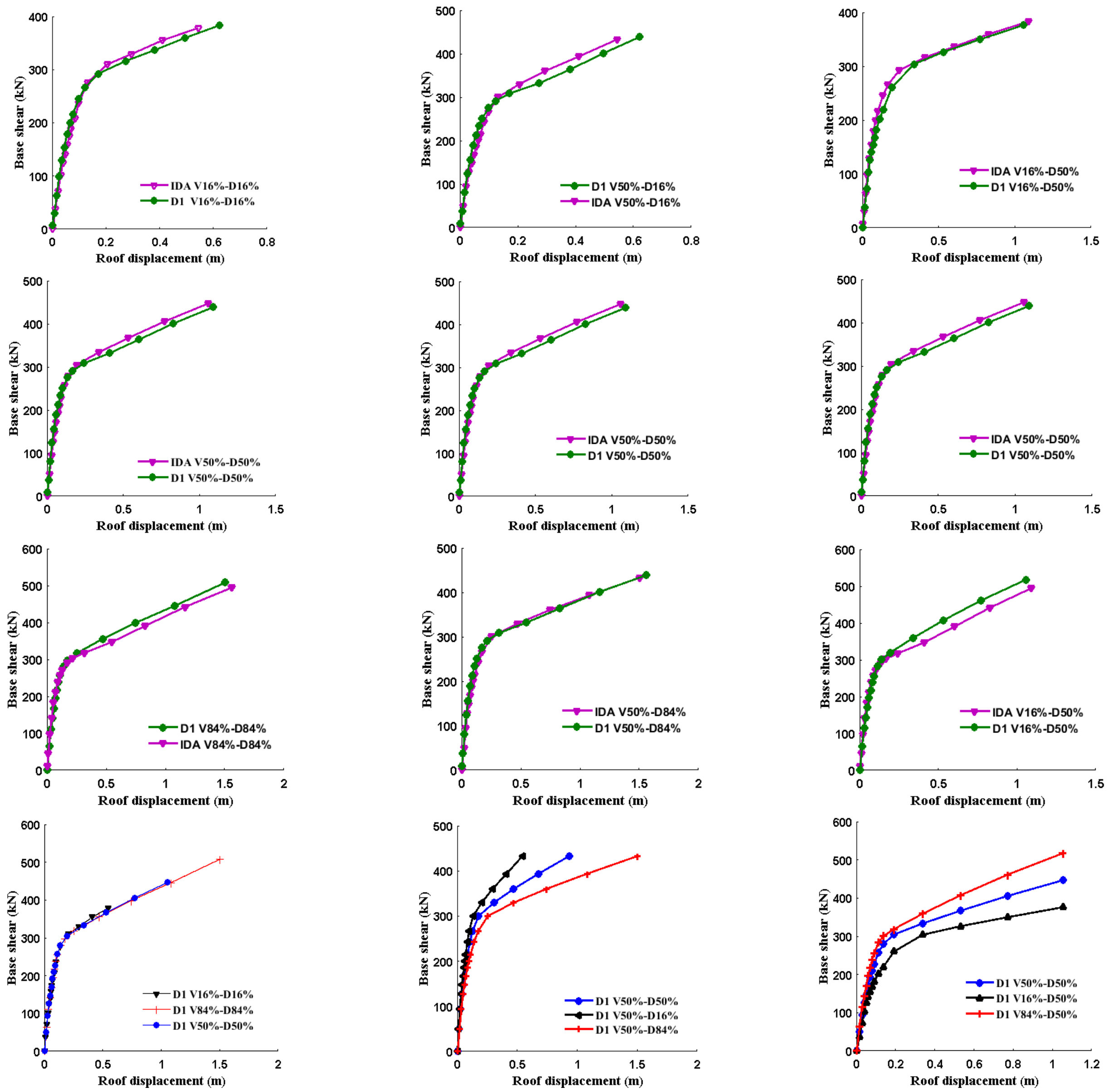

(a) (b) (c)

Fig. 9 Probabilistic capacity curves (D1 stands for linearization method). (a) Both base shear and roof displacement for different percentile, (b) base shear for 50th percentile and roof displacement for different percentile, (c) roof displacement for 50th percentile and base shear for different percentile

be used for the cases where different parts of the structure are intended to be evaluated for different performance levels. For instance, if within the specific structure, the displacement control members are intended to be assessed for 50th percentile and force control members for higher performance level, for example 84th percentile, one can use

Frame1

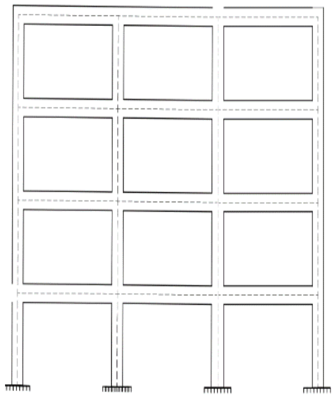

Story height and bay width: 3.2 m & 4.0 m
f_y=400 MPa , f_c=25 MPa

Level	Column size (m)	Column reinf.	Beam size (m)	Beam top & bot. reinf.
1	0.4*0.4	9Φ25	0.3*0.3	5Φ20&5Φ20
2	0.4*0.4	9Φ25	0.3*0.3	5Φ20&5Φ20
3	0.4*0.4	9Φ25	0.3*0.3	5Φ20&5Φ20
4	0.4*0.4	9Φ25	0.3*0.3	5Φ20&5Φ20

Frame2

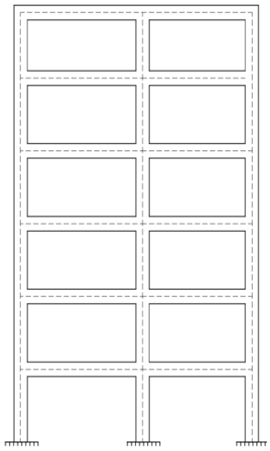

Story height and bay width: 3.0 m & 5.0 m
f_y=400 MPa , f_c=25 MPa

Level	Column size (m)	lumn reinf. C	Beam size (m)	Beam top & bot. reinf.
1	0.5*0.5	12Φ20	0.5*0.5	5Φ20&5Φ20
2	0.5*0.5	12Φ20	0.45*0.45	5Φ20&5Φ20
3	0.45*0.45	12Φ20	0.45*0.45	5Φ20&5Φ20
4	0.45*0.45	12Φ20	0.45*0.45	5Φ20&5Φ20
5	0.45*0.45	12Φ20	0.4*0.4	4Φ20&4Φ20
6	0.4*0.4	12Φ20	0.4*0.4	4Φ20&4Φ20

Frame3

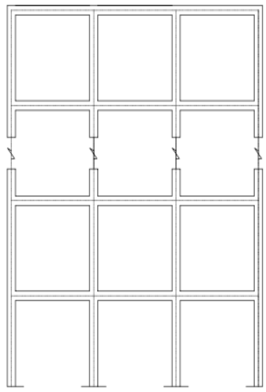

Story height and bay width: 3.0 m & 5.0 m
f_y=400 MPa , f_c=25 MPa

Level	Column size (m)	Column reinf.	Beam size (m)	Beam top & bot. reinf.
1 to 12	0.5*0.5	9Φ25	0.45*0.45	5Φ20&5Φ20

Fig. 10 Geometry of the frames and beam and column cross-sections

the capacity curve type (c).

It is worthwhile to mention that the method is somehow similar to IDA method but instead of conducting several nonlinear analyses at each record intensity, only one linear analysis is performed at each seismic input intensity. Also, in conventional pushover methods the target displacement, which the structure must be pushed to that, is determined by an equation or by using capacity spectrum method in an iterative process and the records uncertainties are not considered. In the proposed method, the structural demand can be computed based on the records frequency specifications and considering record to record uncertainties for any certain confidence level.

3. Validation of the proposed procedure

The proposed pushover procedure is implemented through a computer MATLAB code that uses nonlinear analysis software COM3 (Concrete Model for 3Dimentional problem) (Maekawa 2006, Maekawa *et al*. 2003) for finite element analysis steps.

COM3 is a reinforced concrete-soil foundation oriented FE analysis program developed at Concrete Engineering Lab. of the University of Tokyo.

The SAPA procedure is verified for three 2D frame structures. The responses resulted from the SAPA procedure are compared to those resulted from the IDA and traditional pushover analyses.

3.1 Description of studied structures

As mentioned earlier, three different structures have been considered as case studies; frame1, frame2 and frame3. The configuration and mechanical characteristic of the structure are presented in Fig. 10 the distributed gravity loading on beam elements is equal to 30 kN/m.

In the finite element software, the beams and columns have been modeled with distributed plasticity. Six and ten fiber based element have been considered for each beam and column respectively. Fiber discretization has been used for members section with cyclic nonlinear constitutive laws for concrete and steel bars; the concrete cross section has been divided into confined (core) and unconfined (cover) parts. The multilinear model proposed by Shima *et al*. (2006) has been assumed for reinforcing steel bars. For the concrete, the well-known EPF (elasto-plastic and fracture) model (Maekawa *et al*. 2003) has been assumed.

A set of 30 records of the aforementioned artificial earthquake records have been selected for each frame. The general purpose of the pushover method is to yield the maximum story responses (shear and drift) expected during the earthquake. Therefore, using the information obtained from dynamic analysis (the proposed linearization method) the characteristic of the proper lateral forces which can represent the average of the maximum effect of the ensemble of an earthquake records, can be obtained. Moreover, as it is shown in Fig. 11 the results of the linearization method are in well agreement with IDA analyses even for other probability situations, so if lateral forces other than being representing the average effect of earthquake records is needed, the demands with the corresponding probability should be extracted from the linearization stage of the method.

In Fig. 12, the frames being considered in this study are analyzed with several methods and the resulted interstory drift profiles are compared. As it is obvious the SAPA method result are closer to the dynamic response than the other classic method.

It is observed that for the case of low-rise (four story) frame, interstorey drifts obtained from IDA reach its maximum value at the second story, and it is almost identical to the results of SAPA and inverted triangle constant load profile method. For the case of six story frame, the SAPA method well predict the interstorey drifts obtained from dynamic analysis. For these two low-rise frame case interstorey drift profiles obtained using uniform load profile are somewhat different from those obtained by IDA. On the other hand, for the case of the 12-story frame where the effect of higher mode become more significant, the result of the inverted triangle constant load profile cannot predict the IDA result and at is observed the result of SAPA method are almost identical to IDA result.

As it is shown in Fig. 12 and Table 1 for both values of roof total drift, SAPA method result are closer to IDA result than other push over method.

Also, in Fig. 13 the story ductility demands (μ) of the 12 story frame are compared for the proposed method an IDA method at the same roof displacement demand. The story

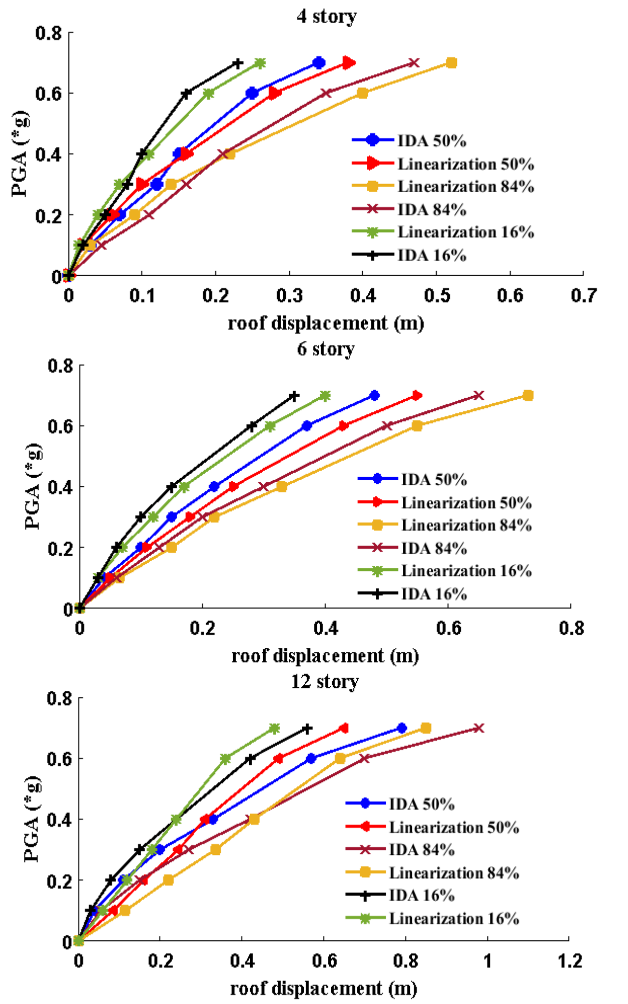

Fig. 11 Maximum roof displacement of the structure for different probability situations

Table 1 Total error of pushover results with respect to IDA interstory drifts

	Frame1		Frame2		Frame3	
Total relative drift (%)	1.5	2.8	1.2	3	1.2	2.5
SAPA (%)	1.28	0.9	1.3	2.43	0.45	1.27
invT. (%)	2.58	1.96	2.27	2.23	1.32	2.93
Uniform (%)	5.12	5.06	4.36	4.69	2.2	1.38

yield displacement was estimated from the idealized force-displacement curve according to ASCE/SEI 41-13 (ASCE 2013).

As it is noticed in Fig. 13, although there is slight deviation in ductility demand in higher intensity records level, the result of the proposed method is still satisfactory.

According to Eq. (57) and the corresponding total drift, the relative difference of pushover results with respect to IDA interstory drifts, has been evaluated in terms of the total error and the results are reported in Table 1.

$$Error_{drift}(\%) = \frac{1}{st}\sqrt{\sum_{n=1}^{st}\left(\frac{{}^{IDA}drift_n - {}^{Linearization}drift_n}{{}^{IDA}drift_n}\right)^2} \tag{57}$$

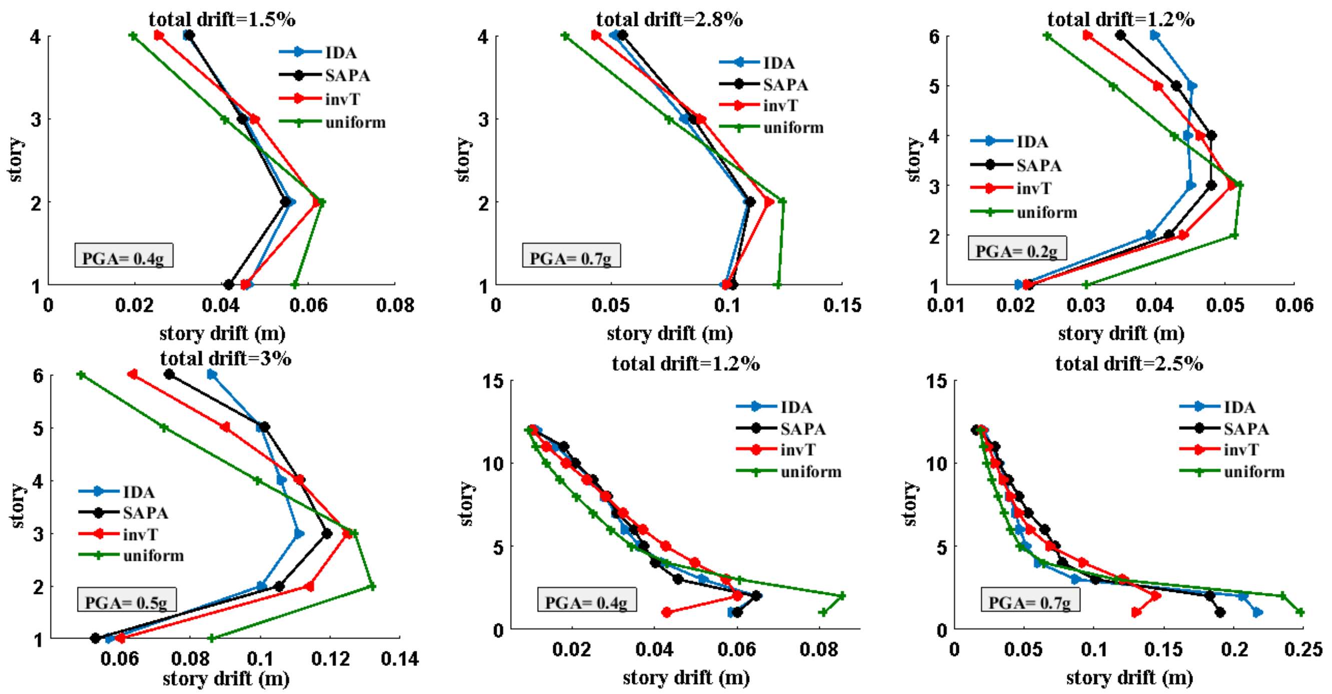

Fig. 12 Story drift profile of the frames from different analysis method

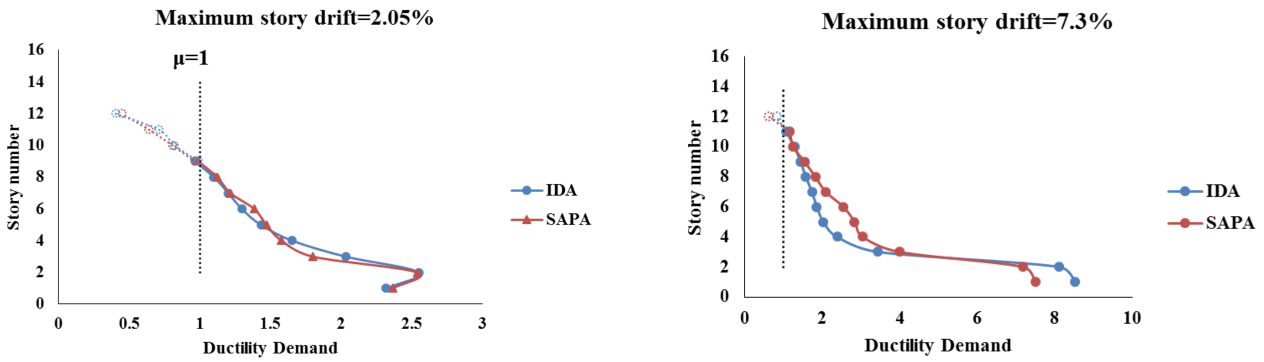

Fig. 13 Story level ductility demand

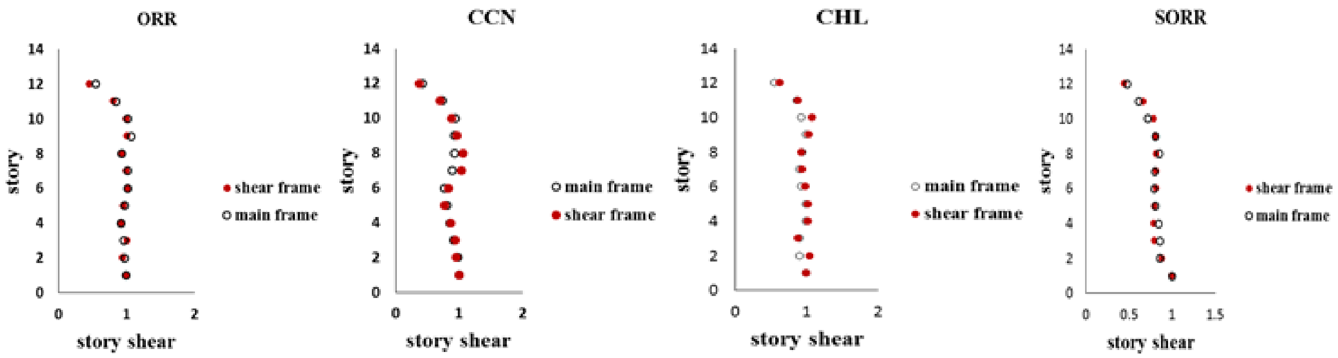

Fig. 14 The comparison of the story shear for idealized shear frame and the main frame

where *st* is the number of the story of each frame.

At this stage of the analyses, the satisfactory of the shear beam idealization reflecting the global behavior of the main model might be unclear. In the proposed method, the shear beam constitutive model is updated and taken from the main structure in each step, which leads to the same lateral force distribution (story shears). In fact, the reason of this idealization is to capture the general behavior of the main structure in the story level scale and truly estimate the changing lateral load profile in different record intensities. When the appropriate lateral load profile is obtained, the shear beam model is put aside and the main model is analyzed under the lateral load and all of the local demands are evaluated.

Story height: 3.2m, $f_{y=}$400 MPa , f_c=30 MPa

Level	Beam size (m)	Beam top & bot. reinf.
1	0.5*0.5	5Φ20&5Φ20
2	0.45*0.45	5Φ20&5Φ20
3	0.45*0.45	5Φ20&5Φ20
4	0.45*0.45	5Φ20&5Φ20
5	0.4*0.4	4Φ20&4Φ20
6	0.4*0.4	4Φ20&4Φ20

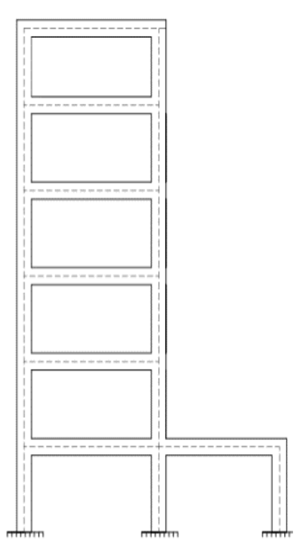

Fig. 15 Frame structure geometry and beam/column cross-sections

Table 2 Maximum rotational ductility demand of the 12 story frame member (the yield rotation of the critical member is θ_y=0.007 (rad))

Total frame drift	2.05%		7.3%	
	IDA (PGA=0.4 g)	SAPA	IDA (PGA=0.7 g)	SAPA
maximum rotation (rad)	0.0197	0.0194	0.07	0.068
maximum rotational ductility	2.81	2.77	10.0	9.71

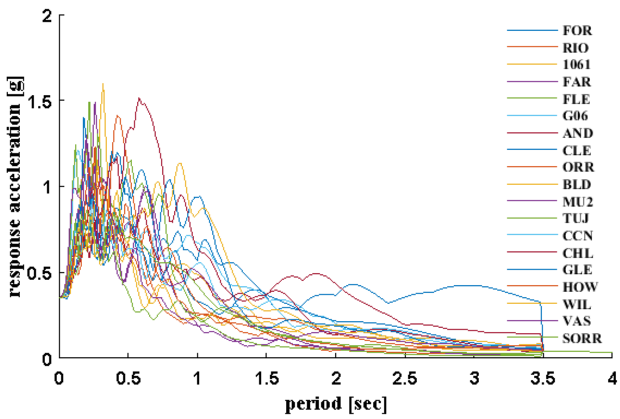

Fig. 16 The acceleration response spectra of the selected records

To verify that the shear beam idealization is able to accurately render the story shear of the main frame under the earthquake records, four separate records mentioned in the following sections with PGA=0.5 g (ORR, CCN, CHL and SORR) were used and nonlinear dynamic analyses were carried out. The story shear (normalized to base shear) versus story level diagram for these records are presented and compared to the results of the proposed shear beam model in Fig. 14. As it shown, the results are close to each other. As stated earlier, once the appropriate lateral load profile is obtained, the shear beam model is put aside and the main model is analyzed under the lateral load and all of the local demands are evaluated. The maximum rotational ductility demand of frame member is one of the main local demand of the frame which might represent the failure initiation. In Table 2, the maximum ductility demands of the critical element within the structure resulted from SAPA method are compared to nonlinear dynamic analyses results and as it is shown the results are in well agreement even near the collapse of structure with story drift ratio of 7.3%. In order to evaluate the local ductility demands, the mean of the maximum total rotation of all elements within the structure were estimated using the total chord rotations. The yield rotation of the member has been estimated from the equivalent multi-linear curve for the diagram of the chord rotation of the element versus moment demand (ASCE 2013).

As another example, a structure with a setback in the second floor has been also evaluated. The configuration and member properties of the structure are shown in Fig. 15. Again masses were considered at the level of beams and the gravity loading on beam elements was equal to 30 kN/m.

19 far-field ground motion records in soil type C have been selected for analysis. The specifications of the selected earthquake ground motion and their acceleration response spectra are presented in Fig. 16 and Table 3.

Since interstory drift plays a crucial role in the amount of damage induced in the structure during earthquake, it is used to assess the accuracy of the proposed pushover method against the nonlinear time history analysis. It seems that the proposed method has better performance in predicting the responses of the dynamic analyses.

According to Fig. 18 and Table 4, the comparison between results shows that:

- In all cases, the result obtained from the proposed method is better matched to IDA results.

- In conventional pushover methods the target displacement which the structure must be pushed to it, is determined by an equation or by using capacity spectrum

Table 3 Specifications and details of the selected records

#	Record ID	Event	*M*	*R* (km)	Soil Type	PGA (g) Component X Y	Selected Component
1	FOR	Cape Mendocino	7.1	23.6	C	0.114 0.116	X
2	RIO	Cape Mendocino	7.1	18.5	C	0.549 0.385	X
3	1061	Duzce	7.1	15.6	C	0.134 0.107	Y
4	FAR	Northridge	6.7	23.9	C	0.273 0.242	X
5	FLE	Northridge	6.7	29.5	C	0.162 0.24	Y
6	G06	Loma Prieta	6.9	19.9	C	0.17 0.126	Y
7	AND	Loma Prieta	6.9	21.4	C	0.24 0.244	X
8	CLD	Loma Prieta	6.9	22.3	C	0.179 0.16	X
9	ORR	Northridge	6.7	22.6	C	0.514 0.568	Y
10	BLD	Northridge	6.7	31.3	C	0.168 0.239	Y
11	MU2	Northridge	6.7	20.8	C	0.444 0.617	X
12	TUJ	Northridge	6.7	24	C	0.245 0.163	Y
13	CCN	Northridge	6.7	25.7	C	0.222 0.256	X
14	CHL	Northridge	6.7	23.7	C	0.185 0.225	X
15	GLE	Northridge	6.7	17.7	C	0.157 0.127	X
16	HOW	Northridge	6.7	20	C	0.163 0.12	Y
17	WIL	Northridge	6.7	25.7	C	0.246 0.136	X
18	VAS	Northridge	6.7	24.2	C	0.139 0.151	X
19	SORR	San Fernando	6.6	24.9	C	0.268 0.324	X

Table 4 Total error of pushover results with respect to interstory drifts obtained by IDA

	Frame 4	
PGA (g)	0.6	0.2
Stochastic (%)	11.2	18.7
Inv.T. (%)	75.8	51.2
Uniform (%)	53.6	21.0

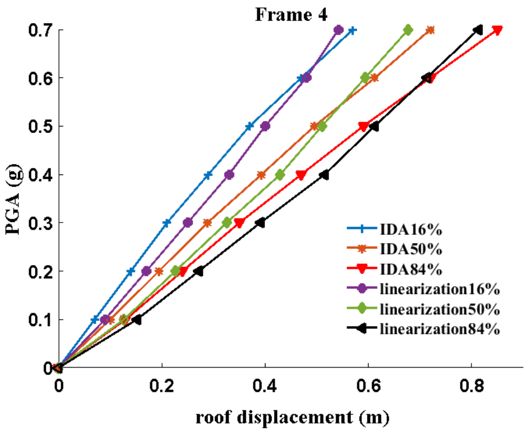

Fig. 17 Maximum roof displacement of the structure for different probability situations

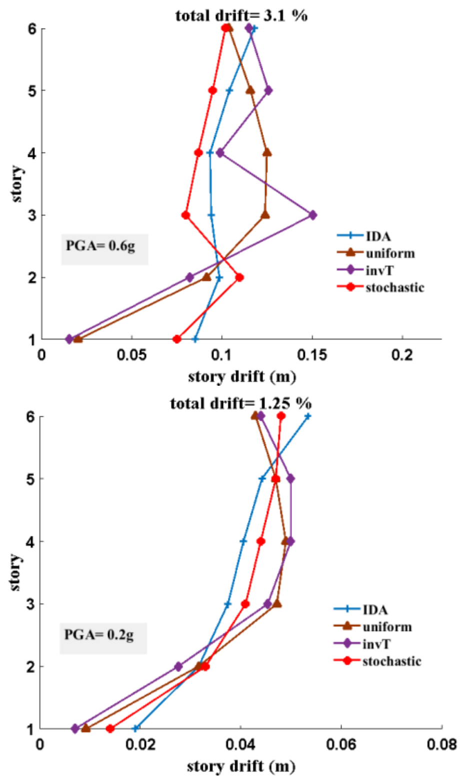

Fig. 18 Story drift profile of the frame 4, obtained from different analysis methods

method in an iterative process and the records uncertainties are not considered. In the proposed method, the structural demand can be computed based on the records frequency specifications and considering record to record uncertainties for any certain confidence level.

- Lateral load distribution is computed and updated in each step and according to what mentioned above, the probabilistic distribution of this load distribution is determined by applying record to record variability.

- The seismic demand of structural components can be computed indeterministicly and for any desired confidence level and any earthquake intensity at each step.

As it is presented in Fig. 17, the results of the linearization method are in well agreement with IDA analyses for different probability situations.

4. Conclusions

Recognizing that most of the proposed pushover analysis cannot directly consider the seismic record uncertainty, by using a stochastic linearization technique, an improved SAPA procedure which takes into account the effects of the higher modes, interaction between modes in the inelastic phase and records uncertainty was presented.

In the proposed procedure, after scaling the base excitation, linearizing the hysteresis system and estimating the demand standard deviations and their derivatives, the extreme value of the demands is estimated by which the lateral force profile is extracted. After verifying the linearization procedure for three structures of 4, 12 and 20 stories, in order to check the accuracy of the proposed procedure, two frame structures were analyzed and the results of the SAPA analysis were compared to dynamic analysis result and other pushover analyses methods. Comparisons show that in all cases the SAPA method better reproduces results of incremental dynamic analysis with respect to conventional procedures based on invariant load vectors.

References

Anagnostopoulos, S.A., Kyrkos, M.T. and Stathopoulos, K.G. (2015), "Earthquake induced torsion in buildings: critical review and state of the art", *Earthq. Struct.*, **8**(2), 305-377.

Antoniou, S. and Pinho, R. (2004), "Development and verification of a displacement-based adaptive pushover procedure", *J. Earthq. Eng.*, **8**(5), 643-661.

Araújo, M., Marques, M. and Delgado, R. (2014), "Multidirectional pushover analysis for seismic assessment of irregular-in-plan bridges", *Eng. Struct.*, **79**, 375-389.

ASCE/SEI 41-13 (2013), Seismic Evaluation and Retrofit of Existing Buildings, Structural Engineering Institute, Reston, VA.

ATC, A. (1996), 40, Seismic Evaluation and Retrofit of Concrete Buildings, Applied Technology Council, Report ATC-40, Redwood City.

Baros, D.K. and Anagnostopoulos, S.A. (2017), "A new approach for 3-D pushover based analysis of asymmetric buildings: development and initial evaluation", *Earthq. Struct.*, **12**(5), 543-557.

Baros, D.K. and Dritsos, S.E. (2008), "A simplified procedure to select a suitable retrofit strategy for existing RC buildings using pushover analysis", *J. Earthq. Eng.*, **12**(6), 823-848.

Beheshti-Aval, S.B. and Keshani, S. (2014), "A Phenomenological study on inelastic torsion caused by nonlinear behavior changes during earthquake excitations", *Civil Eng. Infrastr. J.*, **47**(2), 273-290.

Bouc, R. (1967), "Forced vibration of mechanical systems with hysteresis", *Proceedings of the Fourth Conference on Non-linear Oscillation*, Prague, Czechoslovakia, September.

Bracci, J.M., Kunnath, S.K. and Reinhorn, A.M. (1997), "Seismic performance and retrofit evaluation of reinforced concrete structures", *J. Struct. Eng.*, **123**(1), 3-10.

Charalampakis, A.E. and Koumousis, V.K. (2008), "On the response and dissipated energy of Bouc-Wen hysteretic model", *J. Sound Vib.*, **309**(3), 887-895.

Chopra, A.K. and Goel, R.K. (2002), "A modal pushover analysis procedure for estimating seismic demands for buildings", *Earthq. Eng. Struct. Dyn.*, **31**(3), 561-582.

Davenport, A.G. (1964), "Note on the distribution of the largest value of a random function with application to gust loading", *Proc., Inst. Civil Eng.*, **28**, 187-196.

Elghadamsi, F.E., Mohraz, B., Lee, C.T. and Moayyad, P. (1988), "Time-dependent power spectral density of earthquake ground motion", *Soil Dyn. Earthq. Eng.*, **7**(1), 15-21.

Elnashai, A.S. (2001), "Advanced inelastic static (pushover) analysis for earthquake applications", *Struct. Eng. Mech.*, **12**(1), 51-70.

Foliente, G.C. (1993), "Stochastic dynamic response of wood structural systems", Ph.D. Dissertation, Virginia Tech, Virginia.

Gupta, B. and Kunnath, S.K. (2000), "Adaptive spectra-based pushover procedure for seismic evaluation of structures", *Earthq. Spectra*, **16**(2), 367-392.

Hurtado, J.E. and Barbat, A.H. (2000), "Equivalent linearization of the Bouc-Wen hysteretic model", *Eng. Struct.*, **22**(9), 1121-1132.

Kalkan, E. and Kunnath, S.K. (2006), "Adaptive modal combination procedure for nonlinear static analysis of building structures", *J. Struct. Eng.*, **132**(11), 1721-1731.

Kanai, K. (1957), "Semi-empirical formula for the seismic characteristics of the ground motion", *Bull. Earthq. Res. Inst. Univ. Tokyo*, **35**, 209-325.

Landi, L., Pollioa, B. and Diotallevi, P.P. (2014), "Effectiveness of different standard and advanced pushover procedures for regular and irregular RC frames", *Struct. Eng. Mech.*, **51**(3), 433-446.

Lutes, L.D. and Sarkani, S. (2004), *Random Vibrations: Analysis of Structural and Mechanical Systems*, Butterworth-Heinemann.

Maekawa, K. (2006), "General information for COM3", Version 9.11 in MULTI-COM, Department of Civil Engineering, University of Tokyo.

Maekawa, K., Okamura, H. and Pimanmas, A. (2003), *Non-linear Mechanics of Reinforced Concrete*, CRC Press.

Michaelov, G., Lutes, L.D. and Sarkani, S. (2001), "Extreme value of response to nonstationary excitation", *J. Eng. Mech.*, **127**(4), 352-363.

Pour, H.G., Ansari, M. and Bayat, M. (2014), "A new lateral load pattern for pushover analysis in structures", *Earthq. Struct.*, **6**(4), 437-455.

Poursha, M., Khoshnoudian, F. and Moghadam, A.S. (2009), "A consecutive modal pushover procedure for estimating the seismic demands of tall buildings", *Eng. Struct.*, **31**(2), 591-599.

Pre-standard, F.E.M.A. (2000), Commentary for the Seismic Rehabilitation of Buildings, Report FEMA-356, SAC Joint Venture for the Federal Emergency Management Agency, Washington, DC.

Reinhorn, A.M. (1997), "Inelastic analysis techniques", *Proceedings of the US-Italian Workshop on Seismic Evaluation and Retrofit*, USA, New York City, December.

Roberts, J.B. and Spanos, P.D. (2003), Random Vibration and Statistical Linearization, Courier Corporation.

Sarkar, P., Prasad, A.M. and Menon, D. (2016), "Seismic evaluation of RC stepped building frames using improved pushover analysis", *Earthq. Struct.*, **10**(4), 913-938.

Shayanfar, M.A., Ashoory, M., Bakhshpoori, T. and Farhadi, B. (2013), "Optimization of modal load pattern for pushover analysis of building structures", *Struct. Eng. Mech.*, **47**(1), 119-129.

Tajimi, H. (1960), "Statistical method of determining the maximum response of building structure during an earthquake", *Proceedings of the 2nd WCEE*, 2, 781-798.

Tarbali, K. and Shakeri, K. (2014), "Story shear and torsional moment-based pushover procedure for asymmetric-plan buildings using an adaptive capacity spectrum method", *Eng. Struct.*, **79**, 32-44.

Tataie, L., Brun, M. and Reynouard, J.M. (2012), "Modal pushover procedures for seismic evaluation of reinforced concrete structures: using new nonlinear single degree of freedom systems", *Eur. J. Environ. Civil Eng.*, **16**(2), 178-203.

Vamvatsikos, D. and Cornell, C.A. (2002), "Incremental dynamic analysis", *Earthq. Eng. Struct. Dyn.*, **31**(3), 491-514.

Wen, Y.K. (1976), "Method for random vibration of hysteretic systems", *J. Eng. Mech. Div.*, **102**(2), 249-263.

CC

Appendix

Bouc-Wen parameters of the hysteresis frame are presented in Tables 1-4.

Table 1 B-W parameters of the 20-DOF frame

		story
k_i	m_i	i
kg/cm	kg.sec^2/cm	
50000	35	1
48000	35	2
48000	35	3
48000	35	4
45000	35	5
45000	35	6
45000	35	7
42000	35	8
42000	35	9
42000	35	10
38000	35	11
38000	35	12
38000	35	13
35000	35	14
35000	35	15
35000	35	16
31000	35	17
31000	35	18
31000	35	19
31000	35	20

Table 2 B-W parameters of the 4-DOF frame

		story
k_i	m_i	i
kg/cm	kg.sec^2/cm	
20000	20	1
18000	20	2
16000	20	3
14000	20	4

Table 3 B-W parameters of the 12-DOF frame

		story
k_i	m_i	i
kg/cm	kg.sec^2/cm	
45500	22	1
42000	22	2
38500	22	3
35000	22	4
31500	22	5
28000	22	6
24500	22	7
21000	22	8
17500	22	9
14000	22	10
10500	22	11
7000	22	12

Table 4 The same parameters for all frames

A	1
β (1/cm)	2
γ (1/cm)	-1
α	0/03
n	2
Story height (m)	3/2